Yale 耶鲁大学-南京信息工程大学大气环境中心
Yale-NUIST Center on Atmospheric Environment

A discussion on the paper “Citywide Impacts of Cool Roof and Rooftop Solar Photovoltaic Deployment on Near-Surface Air Temperature and Cooling Energy Demand”

F. Salamanca , published at Springer,21 April 2016

Zhang Yanqing
2016.10.07

OUTLINE

- Introduction
- Methodology
- Results and Discussion
- Conclusions
- Suggestions

01 Introduction

- With the global warming and the extension of city area, the urban heat island effect has become a serious problem of city environment, especially for hot, semi-arid urban environments where summertime cooling demands are excessive.

- Many studies reveal that the large-scale deployment of roofing technologies is an effective means of reducing energy consumption (e.g., Akbari et al. 2009; Oleson et al.2010; Menon etal.2010; Salamancaetal.2012a ; Cotanaetal.2014; Georgescuetal.2014).

01 Introduction

- Other researchers have utilized more advanced parametrizations of solar systems to evaluate regional impacts of large-scale rooftop solar deployment. For instance, sophisticated building energy model forced with weather-based datasets(Scherba et al.2011); offline urban canopy model (Masson et al. 2014).

- We use WRF(3.4.1) coupled to BEP+BEM system characterize the diurnal cycle of near-surface air temperature and citywide air conditioning electricity consumption for Phoenix and Tucson.

02 Methodology

- BEP+BEM: a building energy model integrated into a multilayer building effect parametrization that computes heat exchange between the buildings and the outdoor environment as well as the anthropogenic heating due to air-conditioning systems.

2.1 Parametrization of Rooftop Solar Photovoltaic Panels

The sensible heat flux from a rooftop solar photovoltaic panel to the atmosphere (term H in Eq. 1 below) is computed as the residual term of the following energy balance equation,

$$(1-\alpha_{PV})SW_{Sky}^{downwelling} + LW_{Sky}^{downwelling} - LW_{PV}^{upwelling} + LW_{Roof}^{upwelling} - LW_{PV}^{downwelling} = E_{PV} + H, \quad (1)$$

- α_{PV} : Albedo of the upward face of the solar photovoltaic panels(0.11)
- $LW_{Sky}^{downwelling}$: Downwelling longwave radiation ($W \cdot m^{-2}$) from the sky
- $LW_{Roof}^{downwelling}$: Downwelling longwave radiation ($W \cdot m^{-2}$) reaching a roof covered with solar panels
- E_{pv} : Electricity production ($W \cdot m^{-2}$) of the solar photovoltaic panels
- $SW_{Sky}^{downwelling}$: Downwelling shortwave radiation ($W \cdot m^{-2}$) from the sky

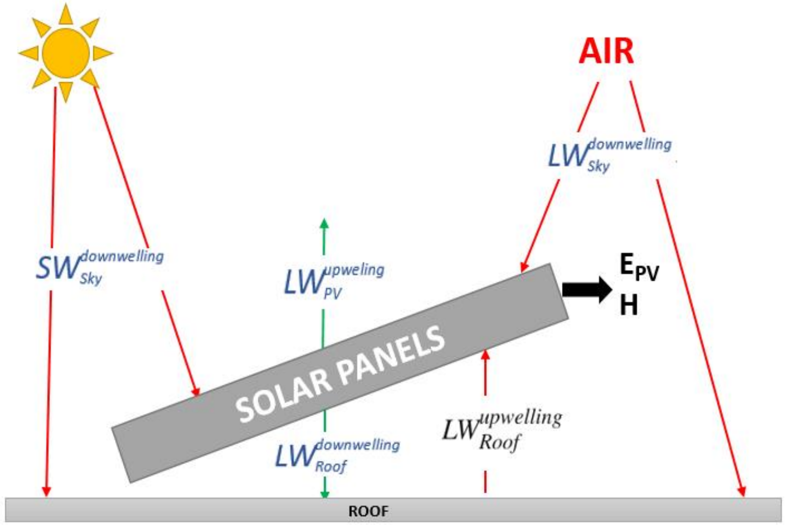

2.1 Parametrization of Rooftop Solar Photovoltaic Panels

其中，

$$LW_{PV}^{upwelling} = \varepsilon_{PV}\sigma T_{PV}^{4} + (1-\varepsilon_{PV})LW_{Sky}^{downwelling}$$

$$LW_{PV}^{downwelling} = \sigma T_{air}^{4}$$

$$T_{PV} = T_{air} + 0.05SW_{Sky}^{downwelling}$$

$$E_{PV} = \varepsilon f f_{PV} SW_{Sky}^{downwelling} \min[1;\ 1-0.005(T_{PV}-298.15)$$

- σ: Stefan-Boltzmann constant ($W \cdot m^{-2} \cdot K^{-4}$)
- $LW_{PV}^{upweling}$: Upwelling longwave radiation ($W \cdot m^{-2}$) emitted by the upward face of the solar photovoltaic panels
- ξ_{PV}: Emissivity of the upward face of the solar photovoltaic panels(0.93)
- T_{PV}: Temperature (K) of the upward face of the solar photovoltaic panels
- $LW_{PV}^{downwelling}$: Downwelling longwave radiation ($W \cdot m^{-2}$) emitted by the downward face of the solar photovoltaic panels
- T_{air}: Air temperature (K) above roofs
- ξff_{PV} Conversion efficiency of the solar photovoltaic panels(0.14)

2.1 *Parametrization of Rooftop Solar Photovoltaic Panels*

The radiative contributions to the surface energy balance of the roof have been modified as follows,

$$SW_{Roof}^{downwelling} = (1 - f_{PV}) SW_{Sky}^{downwelling}, \tag{2}$$

$$LW_{Roof}^{downwelling} = (1 - f_{PV}) LW_{Sky}^{downwelling} + f_{PV} LW_{PV}^{downwelling}, \tag{3}$$

- $SW_{Roof}^{downwelling}$: *Downwelling shortwave radiation ($W \cdot m^{-2}$) reaching a roof covered with solar panels*
- $LW_{Roof}^{downwelling}$: *Downwelling longwave radiation ($W \cdot m^{-2}$) reaching a roof covered with solar panels*
- f_{PV}: *Fraction of the roof covered by the solar panels*

2.2 Numerical Experiments

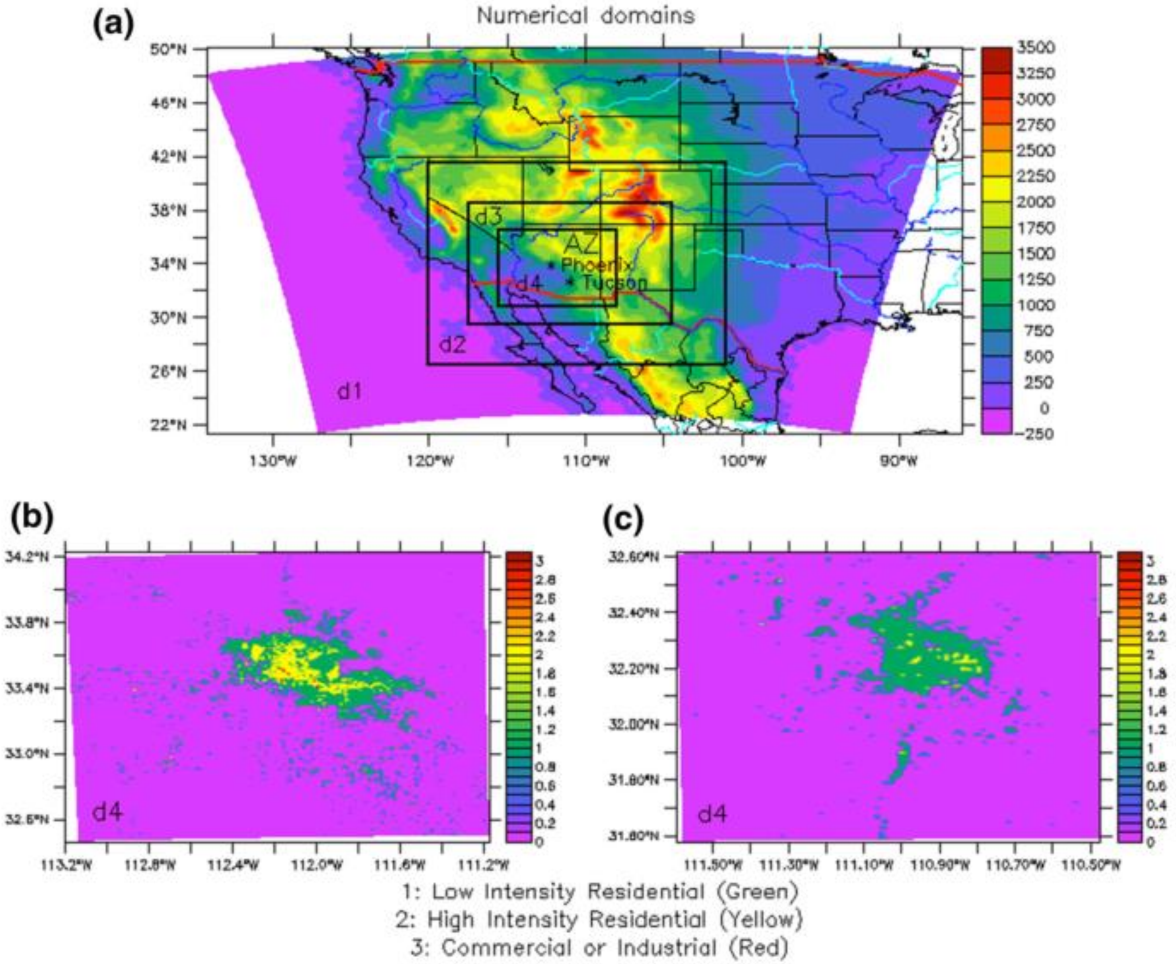

Fig. 1 a The four two-way nested domains used within WRF model experiments. Terrain height is plotted at intervals of 250 m. b Urban classification based on Fry (2011) for the Phoenix metropolitan area. c Same as in (b) but for the Tucson metropolitan area

Experimental period: 10-day clear-sky extreme heat period from July 10 (0000 LT) to July 19 (2300 LT) 2009

Initial and boundary :National Centers for Environmental Prediction Final Analysis data

Four two-way nested domains: 135 × 115 (domain 1), 201 × 183 (domain2), 390 × 321 (domain 3), 615 × 555 (innermost domain) .

Spatial resolutions :27, 9, 3,1 km.

Grid spacing: 1° × 1°.

Temporal resolution:6h.

Urban landscape： US Geological Survey 30-m 2006 National Land Cover dataset (Fry 2011) in the inner domain .

Non-urban: MODIS satellite.

Others :Burian et al (2002) . Clarke et al. (1991)

2.2 *Numerical Experiments*

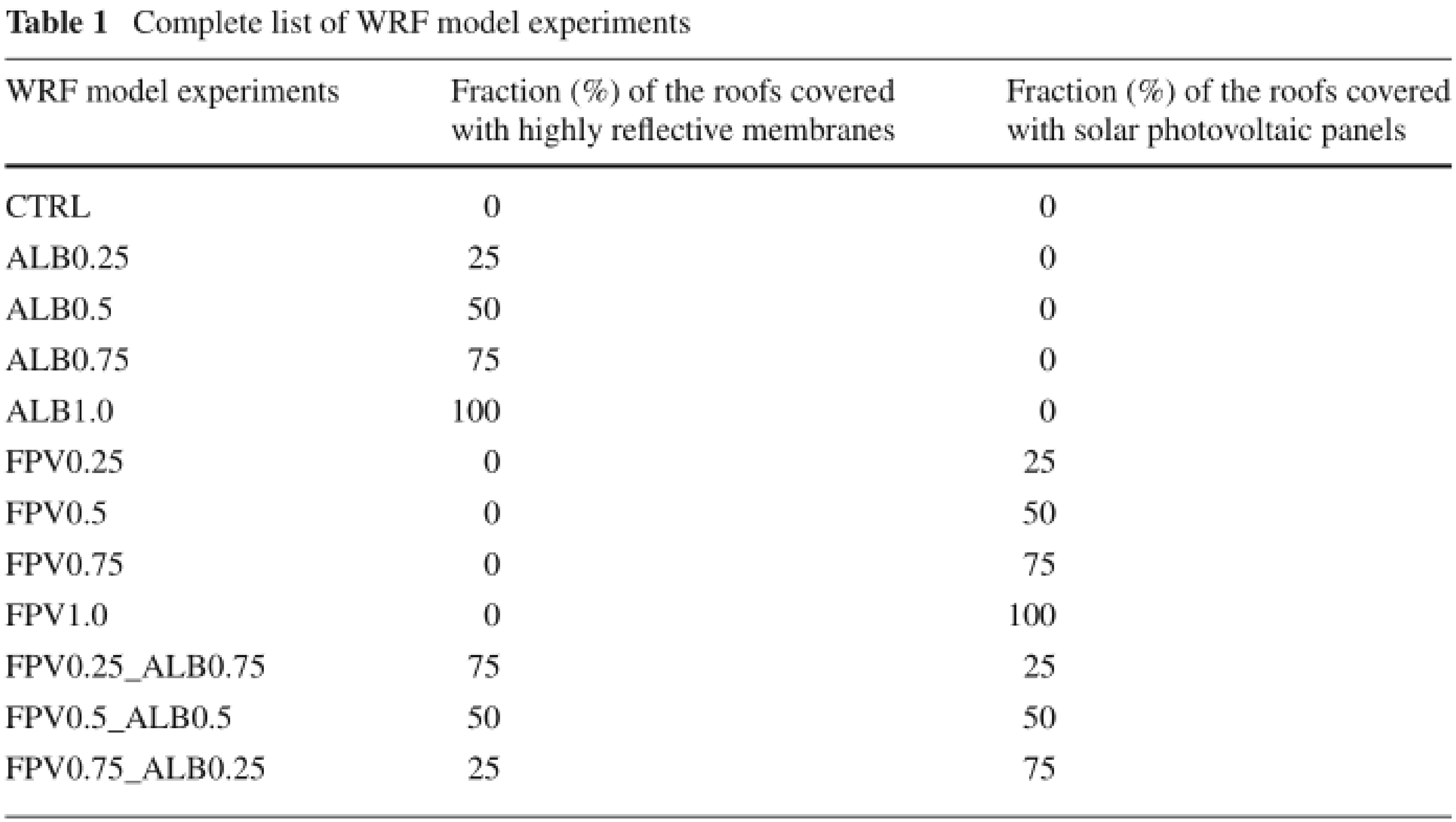

Table 1 Complete list of WRF model experiments

WRF model experiments	Fraction (%) of the roofs covered with highly reflective membranes	Fraction (%) of the roofs covered with solar photovoltaic panels
CTRL	0	0
ALB0.25	25	0
ALB0.5	50	0
ALB0.75	75	0
ALB1.0	100	0
FPV0.25	0	25
FPV0.5	0	50
FPV0.75	0	75
FPV1.0	0	100
FPV0.25_ALB0.75	75	25
FPV0.5_ALB0.5	50	50
FPV0.75_ALB0.25	25	75

e.g. ALB0.75: 75 % of each roof is covered with highly reflective membranes

Albedo of the roofs：CTRL **0.2** , highly reflective surfaces **0.8**

Albedo , emissivity , conversion efficiency of the solar panels :**0.11, 0.93, 0.14**

03 Results and Discussion

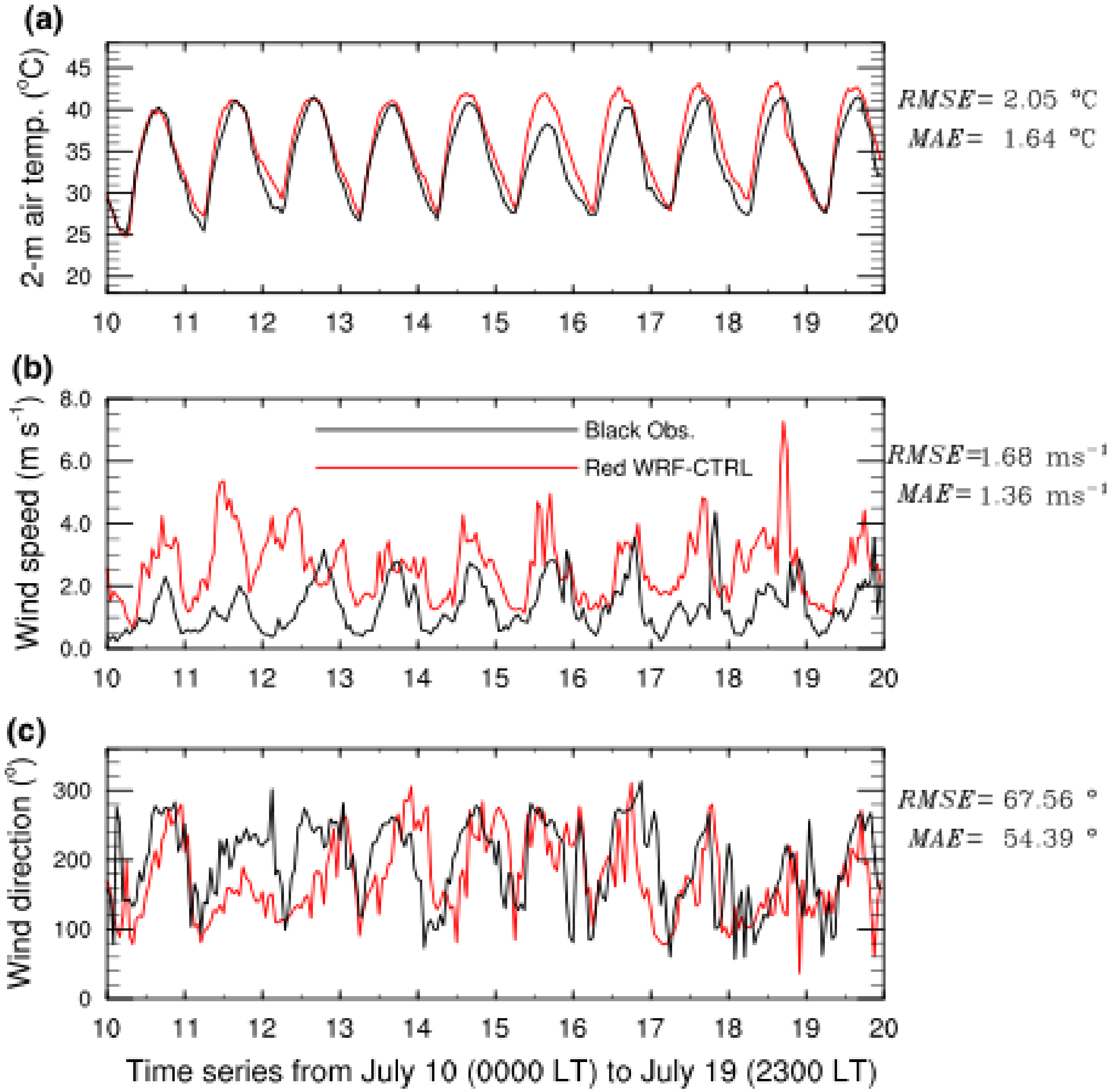

Fig. 2 a Time series of observed (black curve) and CTRL-modelled (red curve) 2-m air temperature (°C) averaged over all six AZMET urban stations (Buckeye, Mesa, Payson, Phoenix Encanto, Phoenix Greenway, and Tucson) during the 10-day extreme heat period in July 2009. b Same as in (a) but for the 10-m wind speed ($m \cdot s^{-1}$). (c) Same as in (a) but for the 10-m wind direction (°). Root-mean-square errors (RMSE) and mean absolute errors (MAE) are also indicated

***3.1** Regional Impacts on Near-Surface Air Temperature*

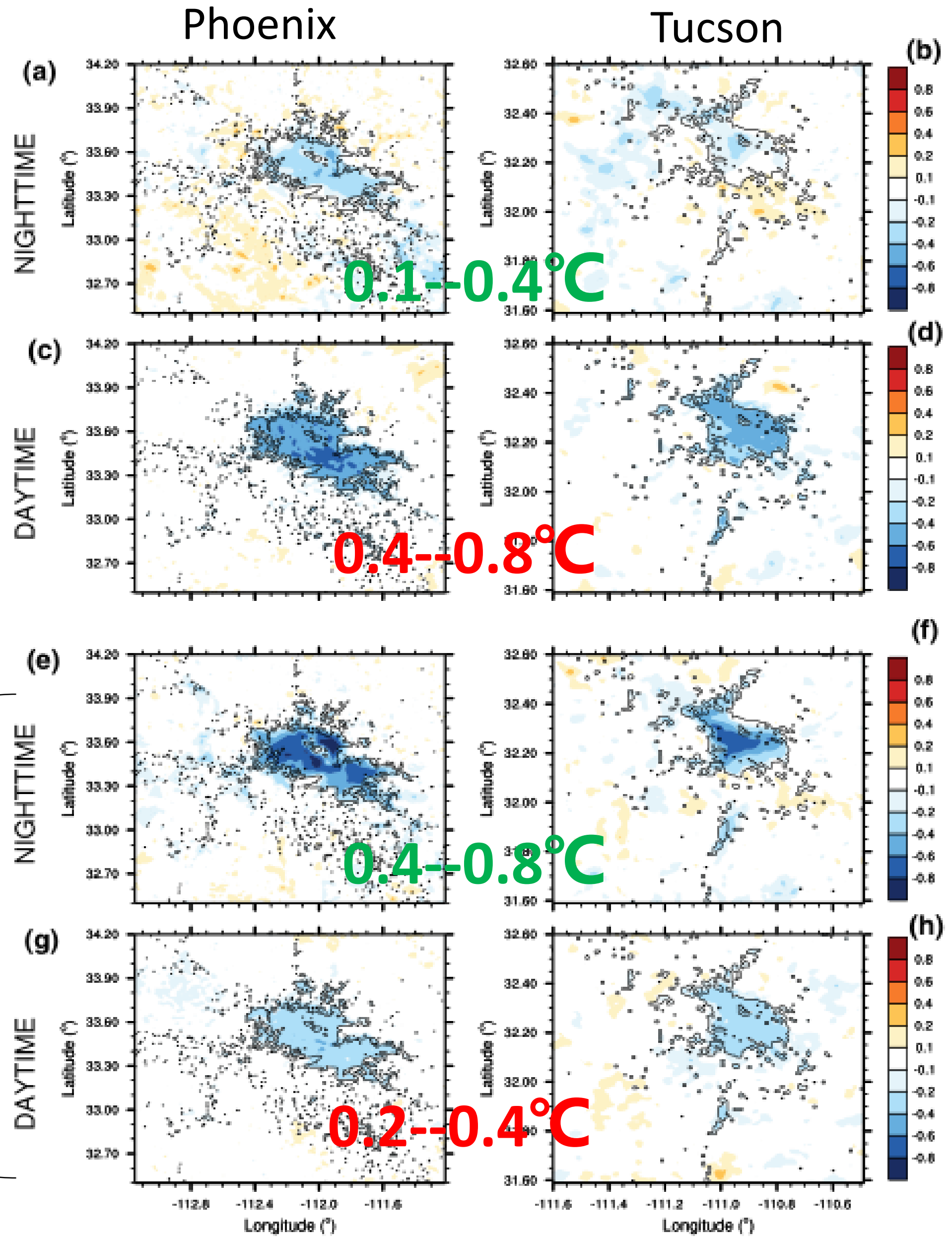

0.1--0.4℃

0.4--0.8℃

0.4--0.8℃

0.2--0.4℃

T_2(ALB1.0)−T_2(CTRL)

T_2 (FPV1.0)
−T_2(CTRL).

Fig. 3 Modelled mean 2-m air temperature differences T_2(ALB1.0)−T_2(CTRL) averaged for the entire 10-day extreme heat period in July 2009 during night time hours (a , b) and during daytime hours (c , d) for Phoenix (left) and Tucson (right) regions, respectively. e–h Same as in (a–d) but for T_2 (FPV1.0)−T_2(CTRL). Urban land use is bounded by black contours.

3.1 *Regional Impacts on Near-Surface Air Temperature*

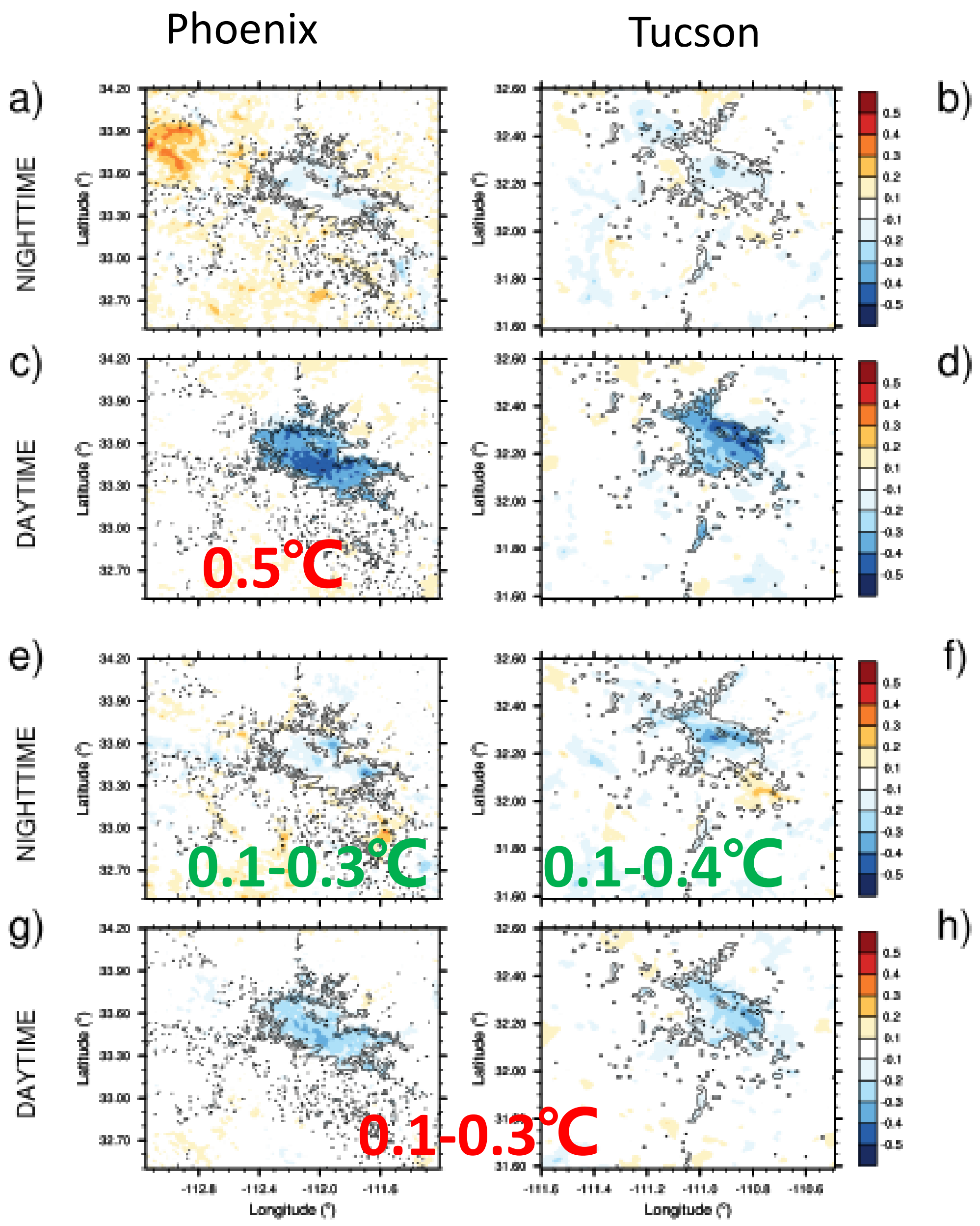

0.5℃

0.1-0.3℃

0.1-0.4℃

0.1-0.3℃

T_2(ALB0.75)−T_2(CTRL)

T_2 (FPV0.75)
−T_2(CTRL)

Fig. S1（in Supplementary material）

3.1 *Regional Impacts on Near-Surface Air Temperature*

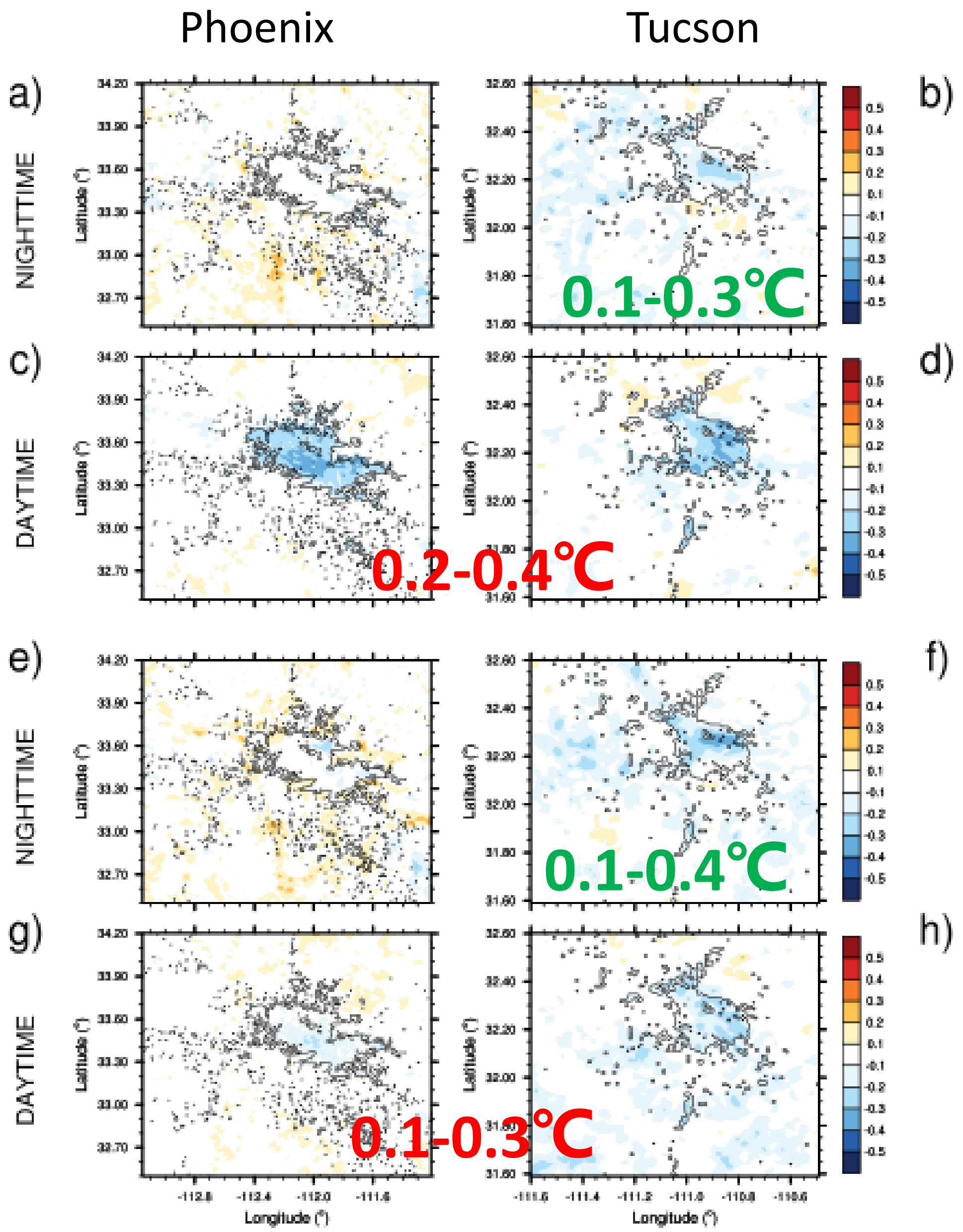

0.1-0.3℃

0.2-0.4℃

0.1-0.4℃

0.1-0.3℃

T_2(ALB0.5)−T_2(CTRL)

T_2 (FPV0.5)
−T_2(CTRL)

Fig. S2（in Supplementary material）

3.1 Regional Impacts on Near-Surface Air Temperature

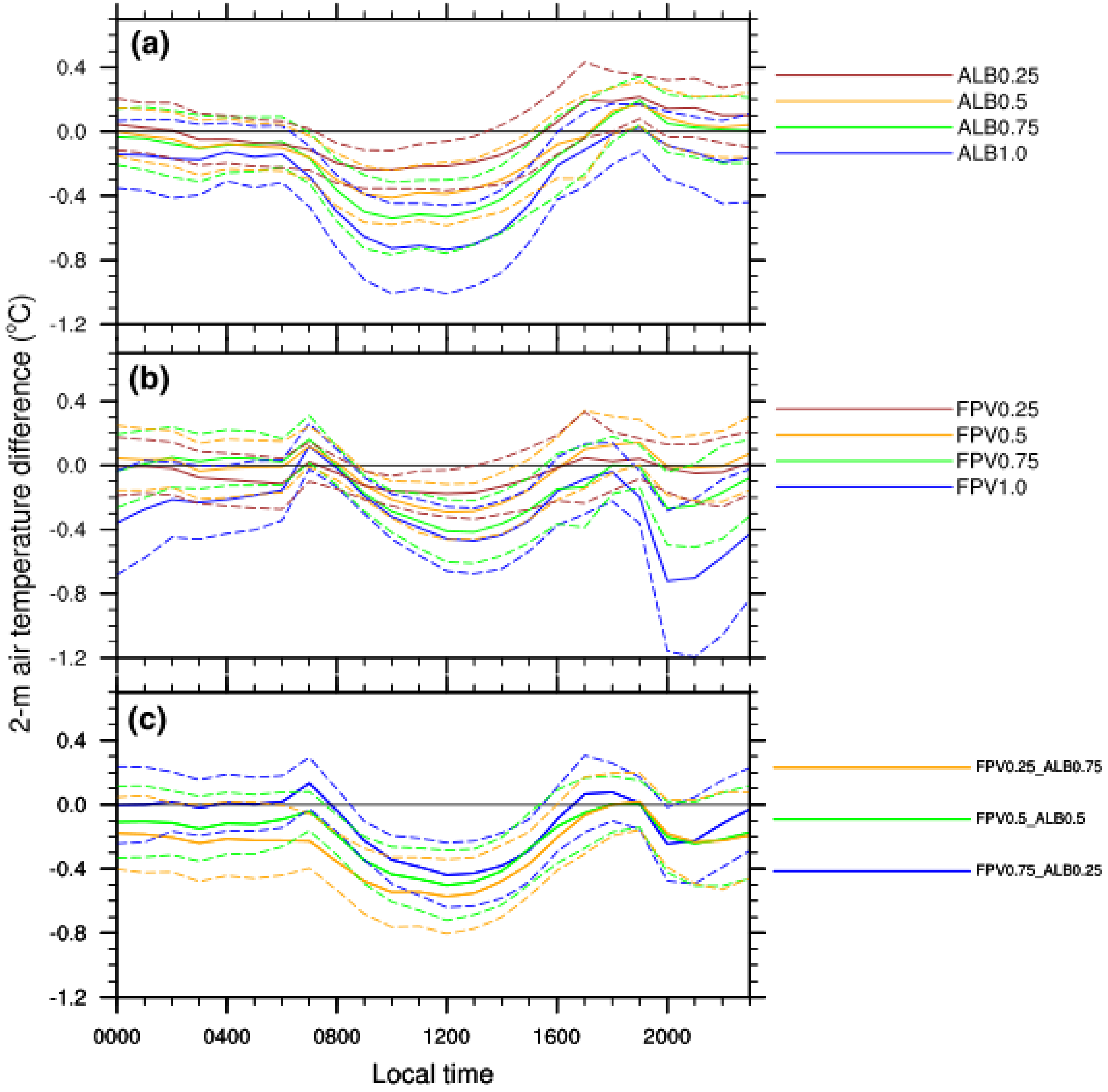

Daytime： 07:00-19:00
Nighttime： 18:00-06:00

Fig. 4 a-c Diurnal cycle of modelled 2-m air temperature differences (we subtracted the CTRL simulation from each WRF model experiment) averaged for the entire 10-day extreme heat period in July 2009 and across the Phoenix metropolitan area for all coverage rates of cool roof deployment. b Same as in (a) but for all coverage rates of rooftop solar photovoltaic deployment. c Same as in (a) but for all the hybrid WRF model experiments. Dashed lines represent ± one standard deviation relative to mean difference showed by the solid curves

3.1 Regional Impacts on Near-Surface Air Temperature

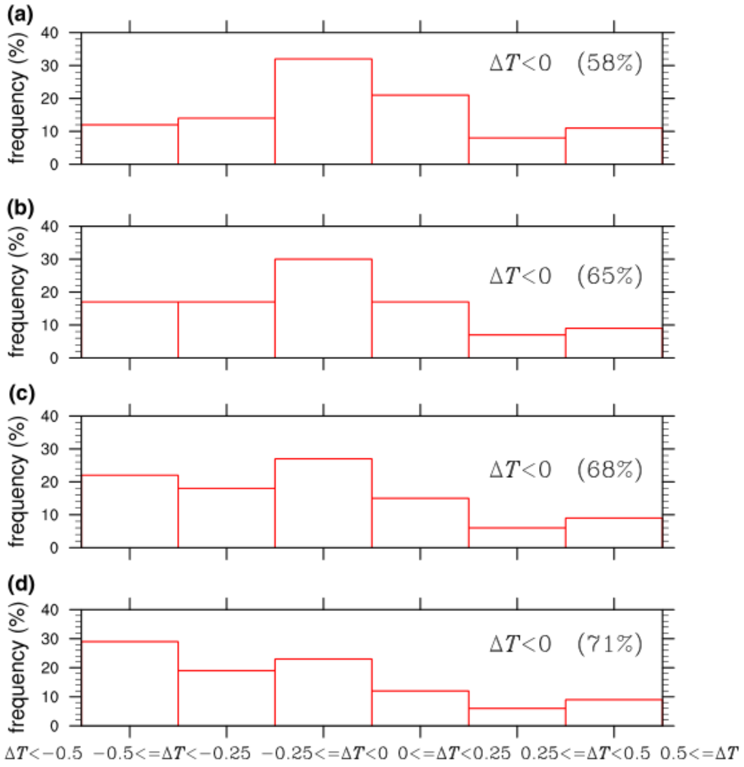

Fig.5 a ,b , c , d： ALB(0.25) 、 ALB(0.5)、 ALB(0.75)、ALB(1.0)

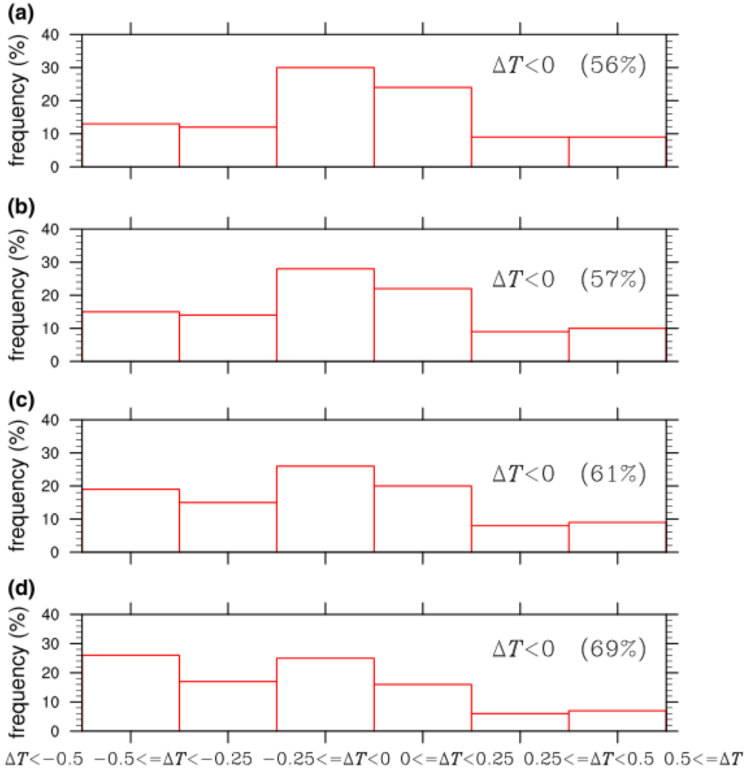

Fig.6 a ,b , c , d： FPV(0.25) 、 FPV (0.5)、 FPV (0.75)、FPV(1.0)

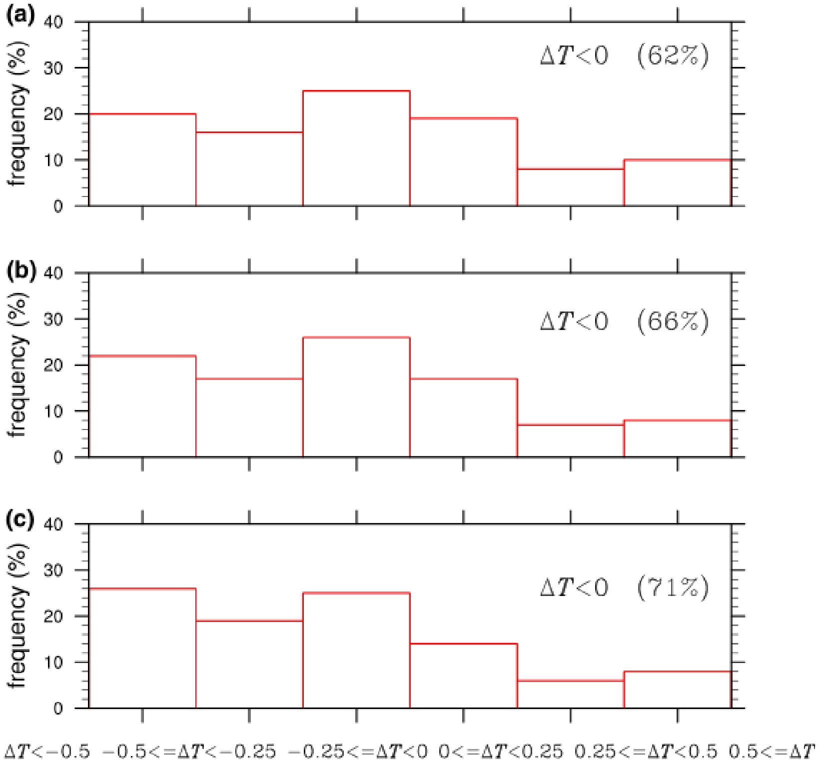

Fig.7 ： FPV(0.75)_ALB(0.25) 、 FPV (0.5)ALB(0.5)、 FPV (0.25)_ALB(0.75)

Fig. 5 ,6 ,7 Bar charts depict the number of times (showed as a frequency in %) that the modelled 2-m air temperature difference [$\triangle T=T_2(WRF)-T_2(CTRL)$] (°C) was in a particular range considering independently each urban grid cell and each hour during the entire 10-day extreme heat period. △T < 0 (XX%) indicates the number of times (in %) that the modelled 2-m air temperature difference was negative.

3.2 Regional Impacts on Cooling Energy Demand

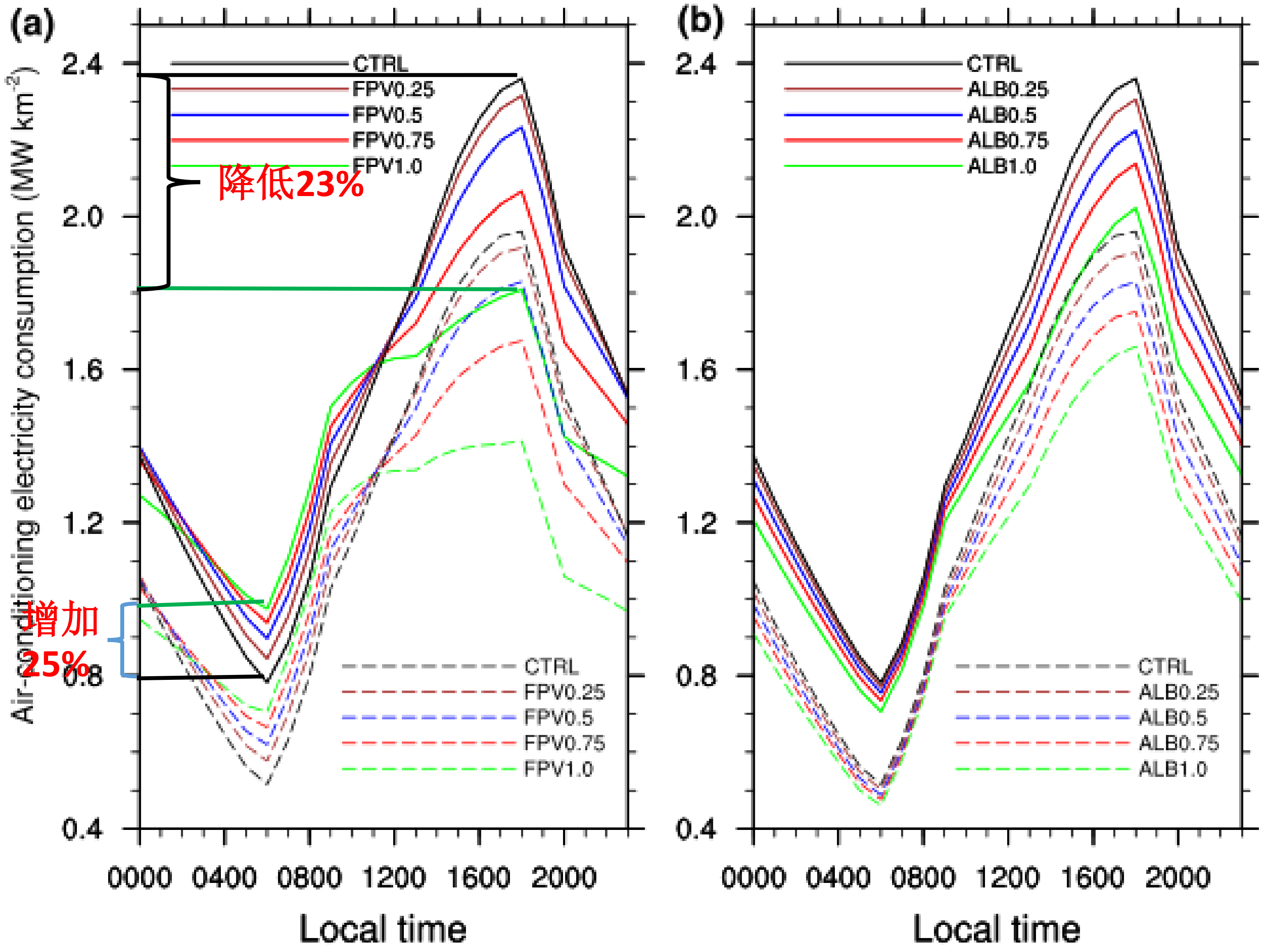

Fig. 8 a Diurnal cycle of modelled air-conditioning electricity consumption (MW km $^{-2}$ of urban land) averaged for the entire 10-day extreme heat period in July 2009 and across the Phoenix (continuous curves) and Tucson (dashed curves) metropolitan areas for all coverage rates of rooftop solar photovoltaic deployment. b Same as in (a) but for all coverage rates of cool roof deployment

3.2 Regional Impacts on Cooling Energy Demand

Table 2 Cooling energy savings across the diurnal cycle (%) and planetary boundary-layer depth reduction (δh) (compared to the CTRL experiment) computed for both Phoenix (PHX) and Tucson (TUC) metropolitan areas

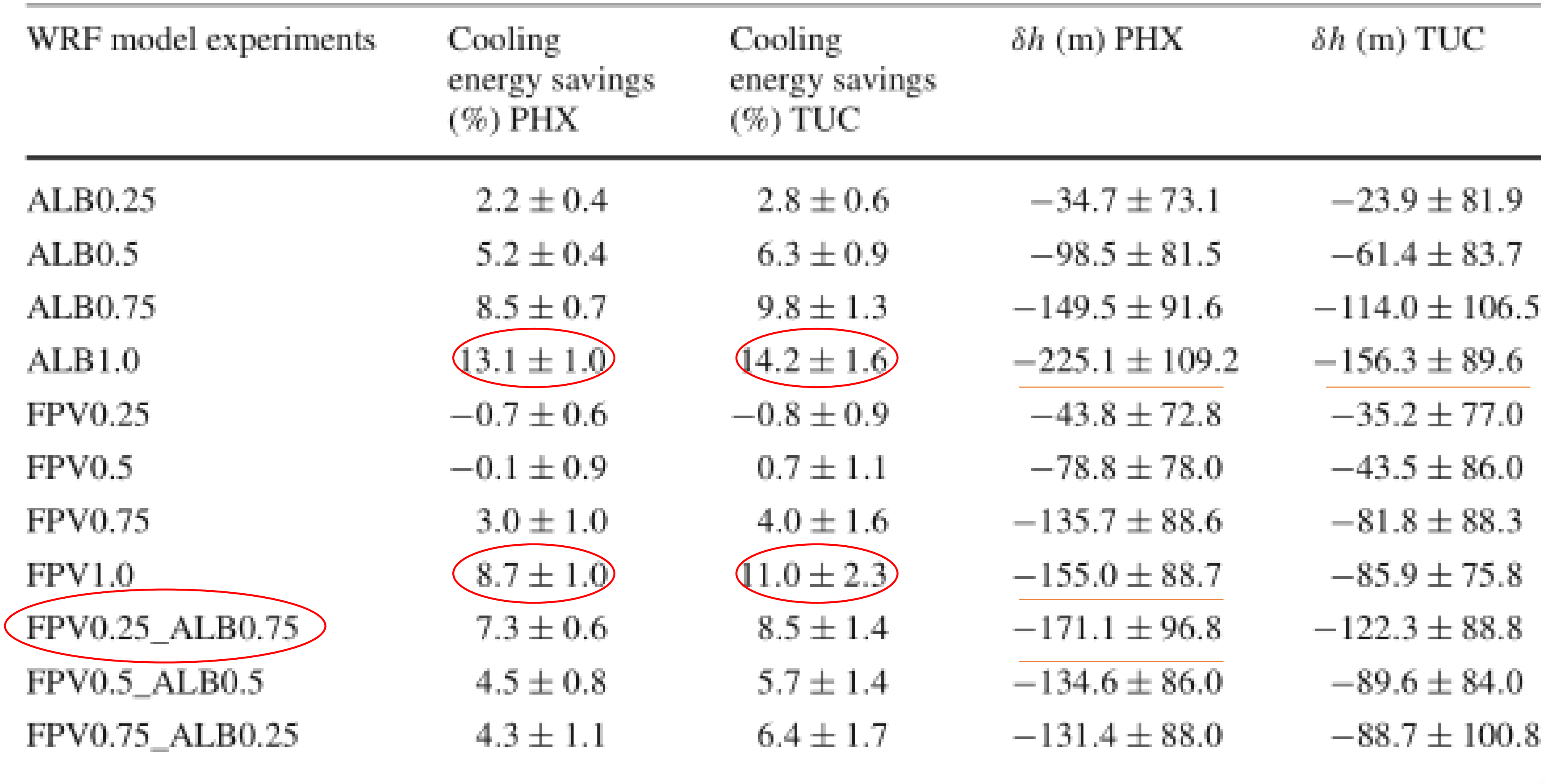

WRF model experiments	Cooling energy savings (%) PHX	Cooling energy savings (%) TUC	δh (m) PHX	δh (m) TUC
ALB0.25	2.2 ± 0.4	2.8 ± 0.6	−34.7 ± 73.1	−23.9 ± 81.9
ALB0.5	5.2 ± 0.4	6.3 ± 0.9	−98.5 ± 81.5	−61.4 ± 83.7
ALB0.75	8.5 ± 0.7	9.8 ± 1.3	−149.5 ± 91.6	−114.0 ± 106.5
ALB1.0	13.1 ± 1.0	14.2 ± 1.6	−225.1 ± 109.2	−156.3 ± 89.6
FPV0.25	−0.7 ± 0.6	−0.8 ± 0.9	−43.8 ± 72.8	−35.2 ± 77.0
FPV0.5	−0.1 ± 0.9	0.7 ± 1.1	−78.8 ± 78.0	−43.5 ± 86.0
FPV0.75	3.0 ± 1.0	4.0 ± 1.6	−135.7 ± 88.6	−81.8 ± 88.3
FPV1.0	8.7 ± 1.0	11.0 ± 2.3	−155.0 ± 88.7	−85.9 ± 75.8
FPV0.25_ALB0.75	7.3 ± 0.6	8.5 ± 1.4	−171.1 ± 96.8	−122.3 ± 88.8
FPV0.5_ALB0.5	4.5 ± 0.8	5.7 ± 1.4	−134.6 ± 86.0	−89.6 ± 84.0
FPV0.75_ALB0.25	4.3 ± 1.1	6.4 ± 1.7	−131.4 ± 88.0	−88.7 ± 100.8

3.2 Regional Impacts on Cooling Energy Demand

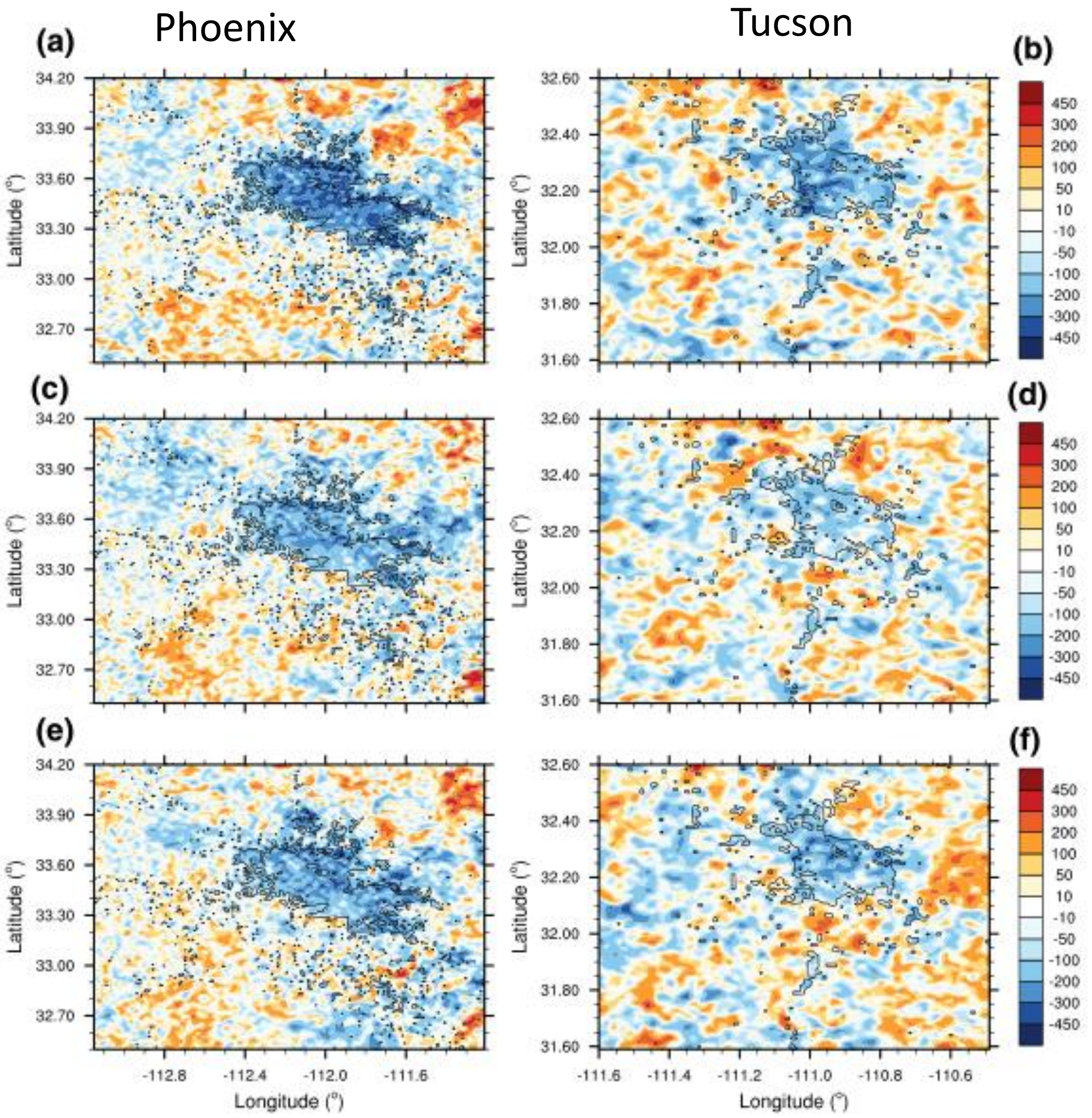

ALB1.0

FPV1.0

FPV0.25_ALB0.75

Fig. 9 a, b Spatial distribution of the modelled PBL height reduction δh(ALB1.0−CTRL) (m) averaged for the entire 10-day extreme heat period in July 2009 for Phoenix (left) and Tucson (right) metropolitan areas. c, d Same as in (a , b) but for δh (FPV1.0−CTRL) . e, f Same as in (a, b) but for δh (FPV0.25_ALB0.75−CTRL) .
Urban land use is bounded by black contours

04 Conclusions

- Our results demonstrate that the deployment of cool roofs and rooftop solar photovoltaic panels reduce near-surface air temperature and cooling energy demand at the scale of the metropolitan area.

- During the day, cool roofs are more effective at cooling than rooftop solar panels, but solar panels are more efficient at reducing the nocturnal UHI magnitude, and therefore more directly combat effects associated with urban development. For the most aggressive coverage rate deployment, cool roofs (rooftop solar photovoltaic panels) lowered mean daytime (nighttime) near-surface air temperature up to 0.8◦C.

- On the other hand, cool roofs are more effective than rooftop solar panels at reducing daily cooling energy demand because solar panels increase nocturnal building-cooling loads. When the maximum coverage rate was considered, the implementation of both roofing technologies reduced daily citywide cooling energy demand by 13–14% for the case of cool roofs, and by 8–11 % for the case of rooftop solar photovoltaic panels.

05 Suggestions

- ✓ potential implications for air quality associated with the reduction of PBL height requires additional investigation to more comprehensively examine the merit of differing strategies.
- ✓ other seasons (e. g .,winter) or other cities in non-semi arid biomes.
- ✓ Morphological differences among various urban areas (e.g., cities with different building plan area fraction, different building sizes, etc) .

THANKS!